Odontology
DOI 10.1007/s10266-016-0232-y

ORIGINAL ARTICLE

Effect of root canal treatment procedures with a novel rotary nickel titanium instrument (TRUShape) on stress in mandibular molars: a comparative finite element analysis

Noemi Bonessio[2] · Ana Arias[1] · Guiseppe Lomiento[3] · Ove A. Peters[1]

Received: 14 October 2015 / Accepted: 23 December 2015

Abstract The aim of this study was to investigate and compare, via finite element analysis (FEA), the effects of endodontic access and canal preparation on stress distribution under functional loading of a mandibular molar treated with novel (TRUShape) and conventional (Vortex) rotary root canal preparation instruments. Identical plastic mandibular molars with natural anatomy had all 4 canals shaped with either TRUShape or a conventional rotary, Vortex (#20 and #30, both by Dentsply Tulsa Dental). Finite element analysis was used to evaluate stress distribution in untreated and treated models. Micro-computed tomography (MCT) of the extracted teeth shaped in vitro was used to inform the FEA model regarding the geometry of root canals and external surfaces. Modeling the intact periodontal support and cancellous/cortical bone was based on anatomical data. Profiles of average and maximum von Mises stresses in dentin of the four treated conditions under functional loading were compared to the untreated model. This comparison was performed for each tooth model with and without root canal obturation and composite restoration. On average, the dentin sections with the most changes after preparation were located in the access cavity, with average stress increase up to +5.7, +8.5, +8.9, and +10.2 % for the TRUShape #20, Vortex #20, TRUShape #30 and Vortex #30, respectively, relative to the untreated model. Within the root canal system, the average stress differences were smaller than <5 % with lower values for TRUShape preparation. A reduction of the average stress in the access cavity was observed as an effect of the composite restoration, while about the same von Mises stress' profiles were found into the root canal. In this finite element analysis, preparation of the access cavity resulted in increased von Mises stresses under functional occlusal load. The limited (up to 0.7 %) retained radicular dentin in the TRUShape versus the Vortex cavity proved effective in reducing masticatory stresses. The bonded restoration modeled in this study only partially counterbalance the combined effects of access cavity and root canal preparation.

Keywords TRUShape · Canal shaping · Finite element analysis · von Mises stress · Root fracture

Introduction

Root canal treatment is a widely used modality to retain teeth that were compromised by deep caries or trauma. However, endodontically treated teeth may be more susceptible to fracture during function [1]. Current understanding indicates that dentin structure and material properties themselves do not change significantly after root canal preparation [2, 3]. Rather, removal of bulk dentin by the incremental restorative procedures is the overriding factor for an increased susceptibility to fracture [4–6]. A variety of nickel titanium (NiTi) instruments are currently used, with minimal differences in terms of volume of the removed bulk dentin. Although any reduction in volume is expected to produce beneficial effects, the quantification of these effects is not trivial. Many factors including root canal shape, relative stiffness of the unaltered portions of the tooth, bone support affect the internal stress distribution that may eventually bring to tooth

✉ Ove A. Peters
opeters@pacific.edu

1 University of the Pacific Arthur A. Dugoni School of Dentistry, San Francisco, CA, USA

2 Department of Mechanical and Aerospace Engineering, University of California, Irvine, CA, USA

3 Department of Civil Engineering, California State Polytechnic University, Pomona, CA, USA

fracture during masticatory functional load. The distribution and magnitude of stresses under masticatory loading, evaluated through finite element analysis (FEA), is a powerful approach that may help to assess a tooth's resistance [7, 8]. In order to properly quantify the stress variation associated with limited differences in a root canal preparation, Micro-computed tomography scans of extracted teeth shaped in vitro can provide accurate 3D root canal geometry for FEA modeling.

Several studies described stress distributions during and after root canal treatment in single rooted teeth [9–15] but only few studies have used FEA to study the mechanical behavior of endodontically treated posterior teeth with complex root canal geometry [16, 17]. In fact the geometrical complexity of root canal's posterior teeth introduces several technical challenges such as MCT scanning resolution, mesh accuracy, and time duration of the FEA analysis.

In this application the FEA method consists of creating idealized digital models of posterior teeth as well as their loads and boundaries in a virtual environment. A major benefit of FEA simulation methods is that different conditions, for example different filling materials, different loads, or different shape and volume of the root canal and/or access cavity may be evaluated non-destructively.

This study was designed to investigate and compare the von Mises stress profiles (maximum and average values) from apex to cusp tip of a mandibular molar after shaping with two different nickel titanium (NiTi) instruments: the novel TRUShape, compared to a nickel titanium rotary instrument with fixed taper (Vortex, both by Dentsply Tulsa Dental Specialties, Tulsa OK, USA).

TRUShape (Fig. 1) is a novel rotary instrument designed with a maximum fluted diameter (MFD) of 0.8 mm in an attempt to reduce coronal shape sizes and preserve bulk dentin. For all TRUShape instruments the taper in the apical 2 mm is 0.06; however, due to a sweeping s-shape in the long axis the instrument can shape canals to a larger envelope of motion if permitted by the canal anatomy [18]. The instrument has a triangular cross-section and a non-cutting tip (Fig. 1b, c). Vortex instruments create a canal shape with a 0.06 taper, which is constant along the length of canal. In that study, the canal geometries created on a sample of extracted mandibular molars showed several differences, notably significantly less removed bulk dentin and also significantly less canal transportation with TRUShape [18].

These findings prompted the underlying hypothesis for this study, which was that retaining radicular dentin by means of minimal reduction in coronal and midroot shaping would translate into appreciable stress reduction in molar teeth under functional load. Micro-computed tomography (MCT) data obtained from extracted teeth shaped in vitro [18] had shown that TRUShape preparation resulted in dentin preservation compared to Vortex shapes. Consequently, in this study data from the MCT scanning are used to inform a FEA simulation, aimed at providing quantitative comparisons between these two instruments in terms of stress distributions in mandibular molar teeth after endodontic access cavities and canal preparation.

Materials and methods

Finite element analysis was selected to evaluate the von Mises stress profile of a molar tooth when treated with two types of rotary NiTi instruments. To create FEA models that have the same preoperative anatomy, two mandibular molars manufactured based on MCT data (TrueTooth #30-001, DEL, Santa Barbara, CA, USA), were selected. A

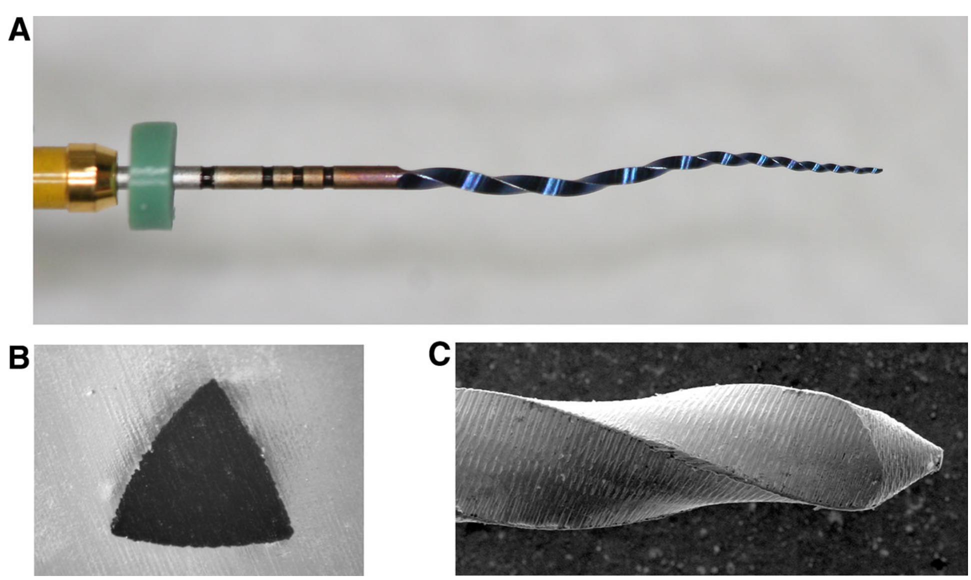

Fig. 1 Overview of the TRUShape instrument in light microscopic and scanning electron microscopic imaging. **a** Instrument with apical size #20. Note the significant s-curve. **b** Cross-section approximately 3 mm from the tip. **c** Tip configuration

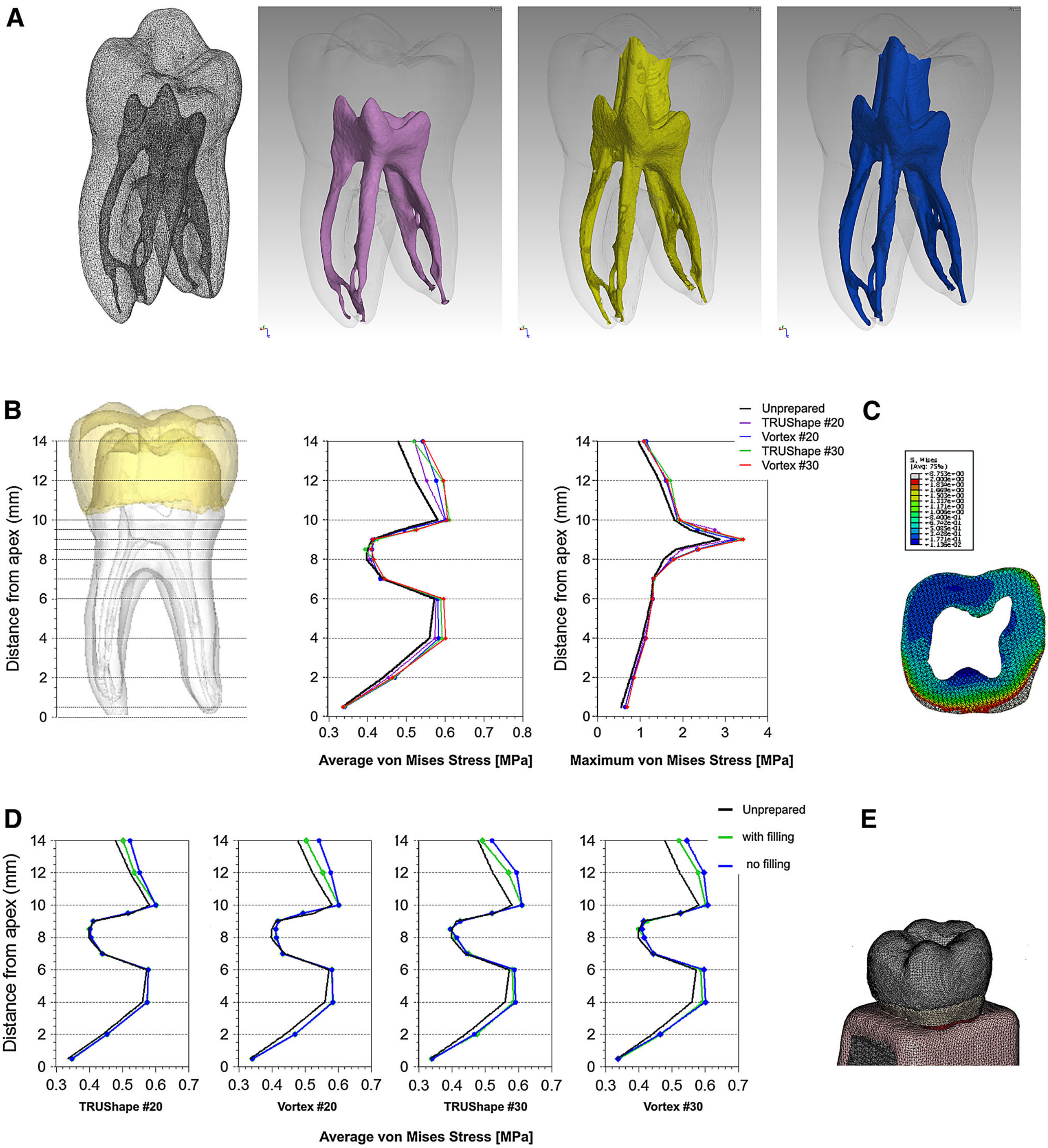

Fig. 2 Finite element analysis of a mandibular molar with realistic canal anatomy prepared with two different root canal preparation instruments. **a** Mesh model and images of canals that are unprepared (*pink*), prepared to size #20 (*yellow*) and size #30 (*blue*), respectively. **b** Location of sections for von Mises stress determination as well as average and maximum von Mises stress profiles at corono-apical levels indicated. Image **c** on *right* shows the 3-dimensional stress distribution 9 mm coronal of the apex. **d** Compares von average von Mises stress profiles of a tooth model with unprepared canals to canals that were prepared, obturated and the access cavity restored with bonded composite. Image **e** to *right* shows the arrangement of models, including tooth, periodontal ligament and bone (color figure online)

third tooth model of identical dimensions was modified so that dentin and enamel of appropriate dimensions could be visualized separately (Fig. 2).

Care was taken to create ideal access cavities for conventional and minimal invasive approaches, prepared by an experienced endodontist (AA). Root canals were then sequentially prepared to apical sizes #20 and #30, and apical tapers of 0.06, with the two selected instruments systems (TRUshape and Vortex, both by Dentsply Tulsa Dental Specialties, Tulsa OK, USA), according to the respective directions for use. Briefly, an experienced endodontist (OP) shaped canals with Vortex after pathfinding and orifice enlargement into the coronal root canal third with an orifice shaper; then a crown down was performed with decreasing sizes of 0.06 taper instruments. Apical shaping was done with sizes #20, #25 and #30 of the same taper. For TRUShape, after pathfinding with K-files, apical preparation was done with instruments size #20 and #30, both of which have a nominal apical taper of 0.06.

Rotaries were powered with an electric motor and manufacturer-recommended settings were selected: 500 rpm and instrument-dependent torque for Vortex and 300 rpm and 3Ncm for TRUShape. Apical patency was maintained throughout the shaping procedures by extending a size #10 K-file (Dentsply Tulsa Dental Specialties) just beyond the apical foramen. Irrigation was with 1 ml water after each file pass, using a 30 g irrigation needle placed as deep as possible into the canal without binding.

MCT scans were then obtained at 20 µm resolution (mCT 50, Scanco, Brüttisellen, Switzerland) before shaping as well as after two shaping steps (sizes #20, #30) in order to obtain four models with shaped canals and one untreated pulp space to use as a reference.

Raw data were imported into VGStudio software (VolumeGraphics, Heidelberg, Germany) and then segmented in an interactive process. Surfaces of outer contours of enamel and dentin, as well as root canal systems, were created and exported as *.stl* files with >50000 triangles. The final FEM models (Fig. 2a) were constructed by importing stereolithography surfaces (enamel, dentin and pulp spaces) into a software platform (ABAQUS, Providence, RI, USA). The enclosed volumes were meshed with 867317 three-dimensional tetrahedral elements and 196144 nodes. The interface was modeled assuming complete bonding. Supporting structures including the periodontal ligament (PDL), cortical bone and cancellous bone were modeled around the tooth root. Thickness of the PDL was assumed as on average 0.2 mm, while the cortical bone was modeled to be about 2 mm based on regular dental anatomy [19, 20]. The size of the supporting bone structure in the mesio-distal and bucco-lingual direction was in agreement with anatomical dimensions of the bone as determined from clinical cone beam tomography (data not shown). The size of the modeled supporting bone segment was reduced with an iterative method. The distance between the cortical bone and the CEJ was about 3 mm, in accordance with normal periodontal conditions [21]. All models were constrained at the external mesio-distal cross-sections of cortical bone and at the apical surfaces of the bone volume.

Table 1 Mechanical characteristics of the materials

Material	Elastic modulus (GPa)	Poisson's ratio
Dentin	18.6	0.32
Enamel	84.1	0.33
PDL	0.0689	0.45
Cortical bone	13.7	0.30
Trabecular bone	1.37	0.30
Gutta percha	0.93×10^{-3}	0.30
Filling composite	14.0	0.30

Different material properties were associated with different portions of the tooth and bone; the Young's moduli (E) and Poisson's ratio (v) values were assigned according to literature data (Table 1). All materials used in this study were assumed to be isotropic and linearly elastic.

A force of 50 N during chewing has been considered typical while force of 500–700 N was considered during parafunctional activity [22]. In the present study typical masticatory function rather than maximum force was to be modeled and therefore a force of 50 N was applied in line of the tooth long axis through a rigid ball (5 mm diameter, assumed as steel), placed onto the occlusal table in contact with the four main cuspal inclines. The contact between enamel and rigid ball was simulated as contact surface. While the current model assumed a single force direction in line with the root long axis, other authors have used 2-step loading cycles between natural occlusal surfaces with a tangential phase prior to maximum intercuspation. Such an analysis is relevant to understand wear patterns, but was not the focus of the current study [23].

A linear static structural analysis was performed to evaluate the stress distribution in the untreated and treated configurations. Specifically, stress distribution and magnitude were computed according to the von Mises definition for effective stress. Results are summarized through average and maximum profile of the von Mises stress in the dentin along the corono-apical dimension of untreated and root canal-treated models.

In dentin each stress profile was built to evaluate the maximum and average value of von Mises stresses in 12 target sections normal to the apical direction and identified by their distance from the apex.

The finite element analyses on the untreated and treated models were conducted in two different configurations with and without root canal filling and coronal restoration. For the restored model, the root canal was filled with gutta percha and sealer, with no bonding assumed. The access cavity was filled with composite assuming perfect bonding to enamel and dentin. The assumed values for Elastic modulus and Poisson's ratio of all implemented materials are given in Table 1.

Results

Shaping to a TRUShape size #20 resulted in dentin removal of 4.2 % of the total dentin volume (1255 mm^3), with a +0.6 % retained dentin in comparison with the 4.8 % volume removal of the Vortex size #20. Similarly, a +0.7 % retained dentin was evidenced for the TRUShape size #30 versus the Vortex size #30, with a dentin volume removal of 4.5 and 5.2 %, respectively.

For all models the maximum stresses were located in the coronal enamel, corresponding to the area of load application and at the contact between enamel and dentin. The profiles of von Misses stress in dentin of all teeth models without root canal obturation and composite restoration are shown in Fig. 2b as average and maximum values, respectively. The trends of average and maximum von Mises stress are similar among the models. The corresponding numerical values of von Mises stresses (average, standard deviation and maximum value) for the access cavity/cervical region (10–12 mm from the apex), coronal third (7–9 mm), middle third (4–6 mm), and apical third (1–3 mm) are reported in Table 2 for the five models, named Untreated, TRUShape size #20, Vortex size #20, TRUShape size #30, and Vortex size #30.

On average, the cervical region/access cavity is predicted to receive, under a 50 N load, stresses ranging from 0.53 to 0.58 MPa, with the smallest and largest values found for the untreated canal space and Vortex size #30, respectively. The corresponding variations of average von Mises stress of the treated models compared to the untreated one are summarized in Table 3.

Stronger effects of the root canal preparation in terms of von Mises stresses in dentin occurred in the access cavity at a distance of 12–14 mm from the apex. With respect to the untreated tooth, the average von Mises stresses after treatment increased by 5.7, 8.5, 8.9 and 10.2 % for the TRUShape #20, Vortex #20, TRUShape #30, and Vortex #30, respectively.

In the root trunk, below the CEJ (coronal third, middle third, and apical third) differences in average stresses between the two sets of instruments were less than <5 % (Table 3). Absolute maximum stresses, in each section of dentin along the corono-apical dimension, increased gradually from the apex to the coronal third, reaching its maximum value of 2.87, 3.16, 3.22, 3.37 and 3.42 MPA (for the untreated, TRUShape #20, Vortex #20, TRUShape #30, and Vortex #30, respectively) in the sections located at a distance of ~9 mm from the apex. Specifically, for those locations the absolute maximum stress occurred in a limited portion of the section at the contact with the cortical bone and corresponding PDL.

In Fig. 2d the profile of each model with root canal obturation and restoration (green line) is plotted together with the profile of the same model but without filling (blue line). Also for comparison purpose the profile of the untreated model (black line) is plotted. The main observed effect of the bonded restoration was a reduction of the average stress in the access cavity, while about the same stresses were found into the root canal region.

Table 3 Von Mises' variation of average values of the treated models TRUShape #20–30 and Vortex #20–30 with respect to the untreated model

	TRUShape #20 (%)	Vortex #20 (%)	TRUShape #30 (%)	Vortex #30 (%)
Access cavity and cervical region	5.68	8.52	8.90	10.23
Coronal third	0.93	2.08	3.47	4.17
Middle third	0.85	1.06	2.55	3.19
Apical third	2.47	4.49	4.72	4.94

Table 2 Von Mises stress (MPa) for access cavity/cervical region, coronal, middle, and apical third

	Untreated	TRUShape #20	Vortex #20	TRUShape #30	Vortex #30
Access cavity and cervical region					
Mean ± SD	0.528 ± 0.051	0.558 ± 0.040	0.573 ± 0.030	0.575 ± 0.049	0.582 ± 0.033
Max	1.81	1.87	1.90	1.90	1.94
Coronal third					
Mean ± SD	0.432 ± 0.046	0.436 ± 0.050	0.441 ± 0.046	0.447 ± 0.066	0.450 ± 0.066
Max	2.87	3.16	3.22	3.37	3.42
Middle third					
Mean ± SD	0.470 ± 0.091	0.474 ± 0.091	0.475 ± 0.091	0.482 ± 0.093	0.485 ± 0.097
Max	1.55	1.71	1.76	1.78	1.79
Apical third					
Mean ± SD	0.445 ± 0.112	0.456 ± 0.120	0.465 ± 0.120	0.466 ± 0.126	0.467 ± 0.132
Max	1.05	1.09	1.13	1.13	1.14

Discussion

To the best of our knowledge this is the first study that uses scanned plastic teeth with natural root canal anatomy to create finite element analysis (FEA) investigating the mechanical response to functional loading. The 5 models were created after shaping with a conventional fixed taper rotary and the novel TRUShape instrument shaped to apical sizes #20 and #30, respectively, along with one uninstrumented negative control model.

Natural teeth were considered but not chosen as the model for the study, because it had been shown that preoperative anatomy is directly associated with shaping outcomes; this was likely to obscure any effect of a shaping with a particular preparation instrument on simulated loading.

Recently the same type of stereolithography-made tooth model with natural canal anatomy was used to visualize root canal irrigation efficacy [24]. It should, however, be kept in mind using stereolithography-made teeth with natural canal anatomy has its own limitations, such as cutting ability of the plastic material. We also considered dimensional variability from sample to sample as a potential confounding factor. However, our pilot studies using an extracted tooth and a stereolithography-produced analog (3D_AE601_19, Acadental, Overland Park, KS, USA) showed that prepared shapes in plastic teeth are essentially the same as shaping outcomes in natural teeth. Moreover, another set of pilot studies using the nominal/actual comparison tool in VGStudio based on MCT images of the 5 plastic teeth used in the current study demonstrated that maximum spatial discrepancy was <1 %. Model estimates based on this finding suggested that resulting stress errors were at least an order of magnitude less. Further studies may use a larger number of plastic teeth than the pair used in this study to include spatial discrepancy into the FEA simulation, also in preparation outcomes within clinicians.

Previous studies had identified root canal shape, dentin thickness, and external root morphology (i.e., canal enlargement), as potential factors that affect root stresses distribution during masticatory loading [25]. Those factors potentially may influence the location and direction of root fracture [1, 4, 6]. The shape of the cavity was already considered as a factor affecting the masticatory stress distribution in another previous study [26], in which the cavity was described in terms of radius of curvature and proximal root concavity, thereby not reflecting the actual root shape. Measurement of the root shape can be further improved by including different ways to assess three-dimensional measures to canal geometry as described earlier [27]. Using validated two-dimensional FEA, Messer et al. suggested that rounded canal profiles will help reduce and more evenly distribute stresses within the root, perhaps, reducing fracture susceptibility [28]. On the other hand, increasing the volume of the pulp space by canal enlargement tended to increase the root stress for masticatory loading [20]. Moreover, the magnitude of radicular stresses was found to be directly correlated with the simulated canal diameter [29]. Conversely, Pitts et al. [30] reported no significant correlations between fracture load and size of the root and Chen et al. observed that canal enlargement resulted in minimally increased maximum von Mises stress [16].

In this study two pairs of teeth after root canal preparation were analyzed, with limited mutual differences in terms of volume and shape of dentin removal. The largest differences between the TRUShape and Vortex were localized in the access cavity while along the root third all the partial volumes of the canal were comparable (data not shown). However, it should be kept in mind that access cavity designs followed pertinent clinical recommendation for each rotary system. It has been shown previously that access cavity size is relevant factor for facture resistance of molars and premolars [31].

The present study interrogated the systems in response to 50 N masticatory load; hence the stress magnitudes and distributions were representative of a low deformation range (i.e., far from reaching the fracture limit). The results of the structural analysis are reported in terms of average and maximum Von Mises stress along the height of the root, since they were shown to be related to premature fatigue failure [32]. Average and maximum von Mises stresses along the corono-apical dimension of untreated and root canal-treated models provide a comprehensive comparison between different treatments. Maximum and average stress profiles provide different information about the stress conditions of each section along the tooth. The former represents maximum localized stress values, disregarding the average stress condition of each section, while the latter represents the average stress in each section, disregarding any local stress concentrations.

In detail and in agreement with a recent study [16], maximum stress variations in dentin occurred at the cervical level and access cavity at a distance of 12–14 mm from the apex. Those differences, due to their locations, account for actual volume and shape differences in the access cavity between the two models. The +0.6 % retained dentin of the TRUShape size #20 versus the Vortex #20 cavity reduced von Mises stress increments from +8.5 to +5.7 %. Similarly, the TRUShape size #30, with a +0.7 % retained dentin in comparison with the Vortex size #30, caused von Mises stresses increases up to +8.9 %, lower than the +10.2 % of the Vortex size #30.

In the root canal (coronal third, middle third, apical third) the differences in terms of average stress between the two sets of instruments were limited (<5 %). For example, in the apical third the difference of average stress values between Vortex and TRUShape size #20 instruments is slightly higher than the same difference between Vortex versus TRUShape size #30 instruments. Conceptionally, this finding may be associated with the differences found in the apical third in terms of canal shape.

Fracture development in radicular dentin is a vexing clinical problem. There is some evidence that dental procedures, such as canal preparation and obturation may contribute to this phenomenon [33]. Dentin on the other hand, due to its macro and microstructure, seems to possess fracture-limiting properties [34, 35]. Chewing forces and loading during parafunctional action may also contribute to tooth fracture, specifically after coronal and intraradicular procedures. The additive effect of incremental enamel and dentin removal is well established in the literature [4–6].

The specific combination of several factors, such as shape and size of the access cavity, shape and size of the root canal, and external morphology of the entire tooth may affect root stress distribution under masticatory function. Finite element analysis of a three-dimensional tooth, built with the complex geometry scanned from the actual treated tooth, is an effective way to evaluate the effect produced by all these combined factors on the tooth structural performance. Therefore, while taking the limitations of this approach into consideration, further research using a larger number of teeth is required to pinpoint possible clinical ramifications. For example, the forces applied in the current study are physiologic biting forces in the posterior dentition, while parafunctional forces may be as high as 700 N [4, 36]. Of note, these forces are well below those required to fracture teeth with conservative access cavities [31]. Also, considering the non-linear stress response of dentin to forces higher than those used in the current exploratory study will help to extend the results to understand conditions for enamel and dentin fracture. Finally, other factors to consider are: degradation of dentin [34] repeated application of various levels of load [37] and other forms of restorations.

Within the limitations of the present finite element analysis the following conclusions may be drawn: even limited retaining radicular dentin (by means of reduced coronal and midroot shaping) will reduce von Mises stress under normal functional occlusal load. Preparation of an access cavity resulted in increased von Mises stresses and the bonded restoration modeled in this study did not reduce the stresses to the levels of the intact tooth. However, the results of the present in vitro study need to be extended to understand potential clinical implications.

Compliance with ethical standards

Conflict of interest This study was financially supported by Dentsply Tulsa Dental Specialties, for which entity Dr. Ove Peters serves as a consultant.

References

1. Lertchirakarn V, Palamara JE, Messer HH. Patterns of vertical root fracture: factors affecting stress distribution in the root canal. J Endod. 2003;29:523–8.
2. Cheron RA, Marshall SJ, Goodis HE, Peters OA. Nanomechanical properties of endodontically treated teeth. J Endod. 2011;37:1562–5.
3. Sedgley CM, Harold H, Messer HH. Are endodontically treated teeth more brittle? J Endod. 1992;18:332–5.
4. Zelic K, Vukicevic A, Jovicic G, Aleksandrovic S, Filipovic N, Djuric M. Mechanical weakening of devitalized teeth: three dimensional finite element analysis and prediction of tooth fracture. Int Endod J. 2015;48:850–63.
5. Reeh ES, Messer HH, Douglas WH. Reduction in tooth stiffness as a result of endodontic and restorative procedures. J Endod. 1989;15:512–6.
6. Lang H, Korkmaz Y, Schneider K, Raab WH. Impact of endodontic treatments on the rigidity of the root. J Dent Res. 2006;85:364–8.
7. Bathe KJ. Numerical methods in finite element analysis. 1st ed. Englewood Cliffs: Prentice-Hall; 1976.
8. Zienkiewicz OC, Taylor RL, Zhu JZ. The finite element method: its basis and fundamentals. 6th ed. Oxford: Elsevier Butterworth-Heinemann; 2005.
9. Reinhardt RA, Krejci RF, Pao YC, Stannard JG. Dentin stresses in post-reconstructed teeth with diminishing bone support. J Dent Res. 1983;62:1002–8.
10. Ko CC, Chu CS, Chung KH, Lee MC. Effects of posts on dentin stress distribution in pulpless teeth. J Prosthet Dent. 1992;68:421–7.
11. Ukon S, Moroi H, Okimoto K, Fujita M, Ishikawa M, Terada Y, Satoh H. Influence of different elastic moduli of dowel and core on stress distribution in root. Dent Mater J. 2000;64:19–50.
12. Yang HS, Lang LA, Molina A, Felton DA. The effects of dowel design and load direction on dowel-and-core restorations. J Prosthet Dent. 2001;85:558–67.
13. de Castro Albuquerque R, Polleto LT, Fontana RH, Cimini CA. Stress analysis of an upper central incisor restored with different posts. J Oral Rehab. 2003;30:936–43.
14. Asmussen E, Peutzfeldt A, Sahafi A. Finite element analysis of stresses in endodontically treated, dowel-restored teeth. J Prosthet Dent. 2005;94:321–9.
15. Nakamura T, Ohyama T, Waki T, Kinuta S, Wakabayashi K, Mutobe Y, Takano N, Yatani H. Stress analysis of endodontically treated anterior teeth restored with different types of post material. Dent Mater J. 2006;25:145–50.
16. Chen G, Fan W, Mishra S, El-Atem A, Schuetz MA, Xiao Y. Tooth fracture risk analysis based on a new finite element dental structure models using micro-CT data. Comput Biol Med. 2012;42:957–63.
17. Dejak B, Mlotkowski A. 3D-Finite element analysis of molars restored with endocrowns and posts during masticatory simulation. Dent Mater. 2013;29:309–17.
18. Peters OA, Arias A, Paqué F. A micro-computed tomography assessment of the canal shaping ability of a novel rotary instrument, TRUShape, in mesial canals of mandibular molars. J Endod. 2015;41:1545–50.

19. Boryor A, Hohmann A, Geiger M, Wolfram U, Sander C, Sander FG. A downloadable meshed human canine tooth model with PDL and bone for finite element simulations. Dent Mater. 2009;25:57–62.
20. Rundquist BD, Versluis A. How does canal taper affect root stresses? Int Endod J. 2006;39:226–37.
21. Gargiulo AW, Wentz F, Orban B. Dimensions and relations of the dentogingival junction in humans. J Periodontol. 1961;32:261–7.
22. Bates JF, Stafford GD, Harrison A. Masticatory function—a review of the literature. III. Masticatory performance and efficiency. J Oral Rehabil. 1976;3:57–67.
23. Benazzi S, Kullmer O, Grosse IR, Weber GW. Using occlusal wear information and finite element analysis to investigate stress distributions in human molars. J Anat. 2011;219:259–72.
24. Versiani MA, De-Deus G, Vera J, Souza E, Steier L, Pecora JD, Sousa-Neto MD. 3D mapping of the irrigated areas of the root canal space using micro-computed tomography. Clin Oral Invest. 2015;19:859–66.
25. Tang W, Wu Y, Smales RJ. Identifying and reducing risks for potential fractures in endodontically treated teeth. J Endod. 2010;36:609–17.
26. Sathorn C, Palamara JE, Palamara D, Messer HH. Effect of root canal size and external root surface morphology on fracture susceptibility and pattern: a finite element analysis. J Endod. 2005;31:288–92.
27. Peters OA, Laib A, Rüegsegger P, Barbakow F. Three-dimensional analysis of root canal geometry by high-resolution computed tomography. J Dent Res. 2000;79:1405–9.
28. Versluis A, Messer HH, Pintado MR. Changes in compaction stresses distributions in roots resulting from canal preparation. Int Endod J. 2006;39:931–9.
29. Ricks-Williamson LJ, Fotos PG, Goel VK, Spivey JD, Rivera EM, Khera SC. A three-dimensional finite element stress analysis of an endodontically prepared maxillary central incisor. J Endod. 1995;21:362–7.
30. Pitts DL, Natkin E. Diagnosis and treatment of vertical root fractures. J Endod. 1983;9:338–46.
31. Krishan R, Paqué F, Ossareh A, Kishen A, Dao T, Friedman S. Impacts of conservative endodontic cavity on root canal instrumentation efficacy and resistance to fracture assessed in incisors, premolars, and molars. J Endod. 2014;40:1160–6.
32. Zarone F, Sorrentino R, Apicella D, Valentino B, Ferrari M, Aversa R, Apicella A. Evaluation of the biomechanical behavior of maxillary central incisors restored by means of endocrowns compared to a natural tooth: a 3D static linear finite element analysis. Dent Mater. 2006;22:1035–44.
33. Bier CA, Shemesh H, Tanomaru-Filho M, Wesselink PR, Wu MK. The ability of different nickel-titanium rotary instruments to induce dentinal damage during canal preparation. J Endod. 2008;35:236–8.
34. Arola D. Microstructure and behaviour of radicular and coronal dentin. Endod Topics. 2012;20:30–51.
35. Ivancik J, Neerchal NK, Romberg E, Arola A. The reduction of fatigue crack growth resistance in dentin with depth. J Dent Res. 2011;90:1031–6.
36. van Eijden T. Three-dimensional analyses of human bite-force magnitude and moment. Arch Oral Biol. 1991;1991(36):535–9.
37. Vukicevic AM, Zelic K, Jovicic G, Djuric M, Filipovic N. Influence of dental restorations and mastication loadings on dentine fatigue behaviour: image-based modelling approach. J Dent. 2015;43:556–67.